JCI insight

Adipocyte-specific loss of PPARγ attenuates cardiac hypertrophy

Xi Fang, … , Ju Chen, Nanping Wang

Research Article   Cardiology   Cell biology

Adipose tissue is a key endocrine organ that governs systemic homeostasis. PPARγ is a master regulator of adipose tissue signaling that plays an essential role in insulin sensitivity, making it an important therapeutic target. The selective PPARγ agonist rosiglitazone (RSG) has been used to treat diabetes. However, adverse cardiovascular effects have seriously hindered its clinical application. Experimental models have revealed that PPARγ activation increases cardiac hypertrophy. RSG stimulates cardiac hypertrophy and oxidative stress in cardiomyocyte-specific PPARγ knockout mice, implying that RSG might stimulate cardiac hypertrophy independently of cardiomyocyte PPARγ. However, candidate cell types responsible for RSG-induced cardiomyocyte hypertrophy remain unexplored. Utilizing cocultures of adipocytes and cardiomyocytes, we found that stimulation of PPARγ signaling in adipocytes increased miR-200a expression and secretion. Delivery of miR-200a in adipocyte-derived exosomes to cardiomyocytes resulted in decreased TSC1 and subsequent mTOR activation, leading to cardiomyocyte hypertrophy. Treatment with an antagomir to miR-200a blunted this hypertrophic response in cardiomyocytes. In vivo, specific ablation of PPARγ in adipocytes was sufficient to blunt hypertrophy induced by RSG treatment. By delineating mechanisms by which RSG elicits cardiac hypertrophy, we have identified pathways that mediate the crosstalk between adipocytes and cardiomyocytes to regulate cardiac remodeling.

Find the latest version:

https://jci.me/89908/pdf

Adipocyte-specific loss of PPARγ attenuates cardiac hypertrophy

Xi Fang,[1,2] Matthew J. Stroud,[2] Kunfu Ouyang,[2] Li Fang,[1] Jianlin Zhang,[2] Nancy D. Dalton,[2] Yusu Gu,[2] Tongbin Wu,[2] Kirk L. Peterson,[2] Hsien-Da Huang,[3] Ju Chen,[2] and Nanping Wang[1,4]

[1]Institute of Cardiovascular Science, Peking University Health Science Center, Beijing, China. [2]Department of Medicine, School of Medicine, UCSD, La Jolla, California, USA. [3]Institute of Bioinformatics and Systems Biology, Department of Biological Science and Technology, National Chiao Tung University, Hsin-Chu, Taiwan. [4]The Advanced Institute for Medical Sciences, Dalian Medical University, Dalian, China.

Adipose tissue is a key endocrine organ that governs systemic homeostasis. PPARγ is a master regulator of adipose tissue signaling that plays an essential role in insulin sensitivity, making it an important therapeutic target. The selective PPARγ agonist rosiglitazone (RSG) has been used to treat diabetes. However, adverse cardiovascular effects have seriously hindered its clinical application. Experimental models have revealed that PPARγ activation increases cardiac hypertrophy. RSG stimulates cardiac hypertrophy and oxidative stress in cardiomyocyte-specific PPARγ knockout mice, implying that RSG might stimulate cardiac hypertrophy independently of cardiomyocyte PPARγ. However, candidate cell types responsible for RSG-induced cardiomyocyte hypertrophy remain unexplored. Utilizing cocultures of adipocytes and cardiomyocytes, we found that stimulation of PPARγ signaling in adipocytes increased miR-200a expression and secretion. Delivery of miR-200a in adipocyte-derived exosomes to cardiomyocytes resulted in decreased TSC1 and subsequent mTOR activation, leading to cardiomyocyte hypertrophy. Treatment with an antagomir to miR-200a blunted this hypertrophic response in cardiomyocytes. In vivo, specific ablation of PPARγ in adipocytes was sufficient to blunt hypertrophy induced by RSG treatment. By delineating mechanisms by which RSG elicits cardiac hypertrophy, we have identified pathways that mediate the crosstalk between adipocytes and cardiomyocytes to regulate cardiac remodeling.

Introduction

PPARγ is a member of the nuclear hormone receptor superfamily. It is predominantly expressed in adipose tissue and plays a role in adipogenesis as well as whole-body lipid metabolism and insulin sensitivity (1, 2). The synthetic agonist rosiglitazone (RSG) has been successfully used in the clinical setting to treat type 2 diabetes by acting as an insulin sensitizer. However, adverse side effects, especially those observed in cardiac tissue, have seriously hindered its clinical application (3–6). Recent evidence has suggested that systemic activation of PPARγ by thiazolidinediones induces cardiac hypertrophy in both mouse and rat models (7–11). Cardiac hypertrophy is an adaptive response, in which myocytes grow in length and/or width as a means to increase cardiac pump function and decrease ventricular wall tension (12). Mice overexpressing PPARγ in cardiomyocytes develop cardiomyopathy, suggesting that direct activation of PPARγ in cardiomyocytes may lead to cardiac hypertrophy (13). However, there is evidence to suggest that systemic activation of PPARγ by RSG is able to induce cardiac hypertrophy and oxidative stress in mice that lack PPARγ in cardiomyocytes (7, 14), implying that cardiac effects of RSG may be partially independent of PPARγ in cardiomyocytes. The foregoing implies that activation of PPARγ in noncardiac tissue(s) may contribute to cardiac hypertrophy. However, the candidate tissue(s) responsible for RSG-induced cardiac hypertrophy is unknown.

Healthy adipose tissue plays a cardioprotective role, while dysfunctional adipose tissue may directly or indirectly contribute to cardiomyopathy, including ventricular dilation, myocyte hypertrophy, cardiac inflammation, and systolic dysfunction (15, 16). These data suggest a functional interplay between adipose and cardiac tissues. Given that adipose tissue is a major site of PPARγ expression and function, it is possible that RSG-induced cardiac hypertrophy might be related to PPARγ activation in adipocytes. As well as being important for PPARγ signaling, adipose tissue plays critical roles as an

Table 1. Echocardiographic measurements of Ctrl and AKO mice following RSG treatment for 4 weeks

	BW (g)	IVSd (mm)	IVSs (mm)	LVPWd (mm)	LVPWs (mm)	LVMd (mg)	FS (%)
Ctrl + vehicle	23.4 ± 1.8	0.63 ± 0.02	0.92 ± 0.07	0.60 ± 0.02	1.05 ± 0.13	61.1 ± 11.0	34.7 ± 4.4
Ctrl + RSG	23.8 ± 1.1	0.74 ± 0.08[A]	1.08 ± 0.10 [A]	0.69 ± 0.06 [A]	1.11 ± 0.03	87.4 ± 7.2 [A]	32.2 ± 3.4
AKO + vehicle	25.5 ± 2.2	0.69 ± 0.07	0.96 ± 0.08	0.64 ± 0.06	1.05 ± 0.07	74.4 ± 11.1	31.1 ± 5.1
AKO + RSG	23.3 ± 1.8	0.69 ± 0.05	1.02 ± 0.09	0.68 ± 0.05	1.12 ± 0.06	71.1 ± 8.6	41.3 ± 7.0

AKO, adipocyte-specific PPARγ knockout mice; Ctrl, littermate control mice; FS, fractional shortening; IVSd, interventricular septal thickness in end-diastole; IVSs, interventricular septal thickness in end-systole; LVMd, left ventricle mass in end-diastole; LVPWd, left ventricular diastolic posterior wall thickness; LVPWs, left ventricular systolic posterior wall thickness; RSG, rosiglitazone. n = 5–8 mice per group. Data are represented as mean ± SEM; [A]$P < 0.05$ vs. Ctrl + vehicle, according to 2-tailed Student's t test.

endocrine organ, secreting multiple cytokines to regulate systemic energy homeostasis, inflammation, and insulin resistance (17). Interestingly, a recent screen revealed that adipocytes are able to release microRNAs (miRNAs) (18).

miRNAs are a family of highly conserved, small (~22 nucleotide) noncoding RNAs that posttranscriptionally repress gene expression via degradation or translational inhibition of their target mRNAs (19). Many miRNAs have been discovered to play key roles in cardiac remodeling, including miR-1 in attenuating agonist-induced hypertrophy, and miR-208 in promoting cardiac hypertrophy (20–22). In addition, cardiac fibroblast–derived miR-21-3p was recently shown to mediate cardiomyocyte hypertrophy (23) through exosomes. The discovery of circulating extracellular miRNAs in body fluids indicates a role for miRNAs in mediating cell-cell communication between tissues (24–26). Exosomes are the major transport vesicle of circulating miRNAs, allowing miRNA transfer and genetic exchange between cells (23, 27–30).

Given the potential interaction between adipose and cardiac tissue, we postulated that RSG might indirectly affect cardiac hypertrophy through PPARγ activation in adipocytes. Indeed, we found that RSG activation of PPARγ signaling in adipocytes led to expression and secretion of miR-200a in exosomes. Exosomes containing miR-200a targeted cardiomyocytes and specifically activated the mTOR pathway to induce cardiac hypertrophy.

Results

RSG regulates miR-200a levels in adipose and cardiac tissue by distinct mechanisms. As a ligand-activated nuclear receptor, PPARγ binds to PPAR response elements (PPREs) and regulates target gene expression. We initially took a bioinformatics approach to look at miRNA genes that could be potentially regulated by PPARγ. Our in silico analysis predicted that the miR-200 cluster contained 3 conserved PPREs in its upstream region (Supplemental Figure 2A; supplemental material available online with this article; doi:10.1172/jci. insight.89908DS1). miR-200a was abundantly expressed in adipose tissue, while barely expressed in vessel, heart, or skeletal muscle (Supplemental Figure 1), exhibiting a similar expression pattern to that of PPARγ (1, 2). To confirm our in silico findings, we performed chromatin immunoprecipitation assays. We found that PPARγ bound to PPRE1 (1,788 bp upstream of transcription start site [TSS]) and PPRE2 (1,614 bp upstream of TSS) (Supplemental Figure 2B) of the miR-200a locus. These findings led us to hypothesize that PPARγ activation by RSG might regulate expression of miR-200a. To assess this possibility, we treated WT mice with RSG (10 mg/kg/d) for 4 weeks and measured the expression of miR-200a using real-time PCR. In adipose tissue, we found that both mature and primary transcripts of miR-200a (pri-miR-200a) were increased following RSG treatment (Figure 1, A and B). However, in cardiac tissue, RSG treatment increased levels of mature miR-200a, but not pri-miR-200a, implying that PPARγ activation modulated the levels of miR-200a in adipose and cardiac tissue through distinct mechanisms (Figure 1, C and D).

To investigate whether increased levels of mature miR-200a in cardiomyocytes were from an indirect source, we treated isolated neonatal mouse cardiomyocytes with different concentrations of RSG. Indeed, we found that RSG was unable to directly affect miR-200a levels in isolated cardiomyocytes, suggesting that increased miR-200a in the heart following systemic PPARγ activation by RSG originates from a noncardiomyocyte source (Figure 1E). We further investigated regulation of miR-200a by RSG in cultured adipocytes. In 3T3-L1–differentiated adipocytes and primary mouse adult adipocytes, both mature and pri-miR-200a levels were significantly increased by RSG. To test the specific effect of PPARγ
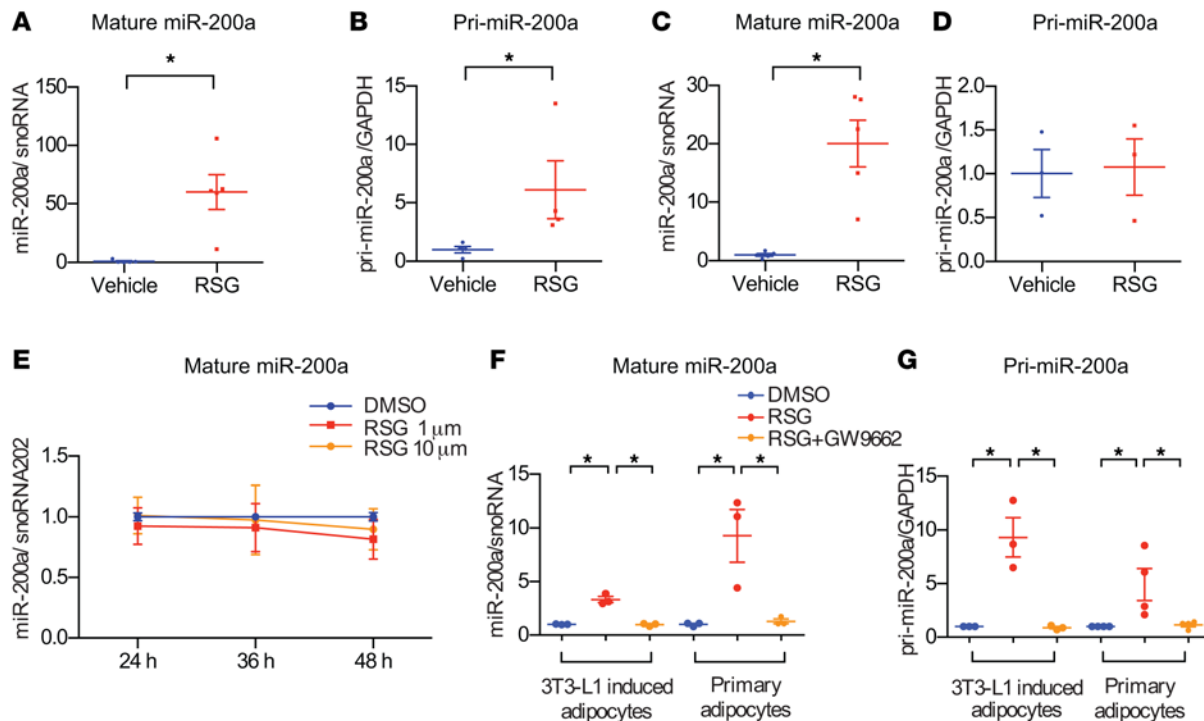
Figure 1. Regulation of miR-200a expression by rosiglitazone. (**A–D**) WT mice were treated for 4 weeks with either rosiglitazone (RSG) or vehicle (control). Levels of mature miR-200a and primary transcript of miR-200a (pri-miR-200a) were quantified using quantitative real-time PCR (qRT-PCR) in adipose (**A** and **B**) and cardiac tissue (**C** and **D**), respectively. Note that miR-200a and pri-miR-200a levels are both increased in RSG-treated adipose tissue, but only mature miR-200a is upregulated in cardiac tissue. n = 5 mice. (**E–G**) Cells were treated with RSG alone, RSG combined with GW9662 (PPARγ antagonist), or DMSO (control). Levels of mature miR-200a and pri-miR-200a were quantified using qRT-PCR. (**E**) Expression levels of miR-200a were measured in cardiomyocytes. Note that miR-200a is not induced in cardiomyocytes by RSG at varying concentrations after 24, 36, and 48 hours of treatment. The experiment was replicated 3 times. (**F** and **G**) Expression levels of miR-200a and pri-miR-200a were quantified in 3T3-L1–induced adipocytes and primary adipocytes treated with RSG alone, RSG combined with GW9662, or DMSO (control). Note that RSG increases both mature miR-200a and pri-miR-200a levels (**F** and **G**, respectively) in both cell types, but the effect is ablated when RSG is combined with the PPARγ antagonist GW9662. The experiment was replicated 3 times. snoRNA 202 and Gapdh were used as internal controls for qRT-PCR experiments. Data are represented as mean ± SEM; *P < 0.05 according to 2-tailed Student's t test for **A–D** and 1-way ANOVA for **E–G**.

activation, we pretreated adipocytes with the PPARγ antagonist GW9662. As expected, we found that the PPARγ antagonist was sufficient to abrogate increases in both mature miR-200a and pri-miR-200a levels in response to RSG treatment in adipocytes (Figure 1, F and G). Together, these results suggested that PPARγ activation by RSG might directly induce miR-200a transcription in adipocytes, potentially indirectly leading to an increase in miR-200a levels in cardiomyocytes.

Exosomes transport miR-200a from adipocytes to cardiomyocytes. Recent studies have revealed that miRNAs can circulate and be delivered to recipient cells via exosomes, targeting gene expression in recipient cells (28–31). We hypothesized that RSG might increase miR-200a in the heart through circulating exosomes derived from adipose tissues. In support of this, we detected elevated levels of miR-200a in sera from mice treated with RSG (Figure 2A). Furthermore, we observed a 3- to 5-fold increase in levels of mature miR-200a in culture media from adipocytes treated with RSG (Figure 2B). The effect of RSG was blunted when the cells were pretreated with the PPARγ antagonist GW9662. To test whether miR-200a was transported in exosomes, we used an exosome biogenesis inhibitor, GW4869, in combination with RSG to see whether miR-200a levels in adipocyte culture media would be affected. As predicted, by inhibiting exosome biosynthesis, we found reduced levels of secreted miR-200a in adipocyte culture media (Figure 2B).

To further characterize miRNA-containing exosomes produced by adipocytes in vitro, we performed transmission electron microscopy (TEM) of isolated exosomes (Figure 2C). TEM revealed that the diameter of exosomes was heterogeneous, but the majority of exosomes had diameters of between 60 and 100 nm. In addition to TEM, we also analyzed the contents of isolated exosomes and found that they contained elevated levels of miR-200a when adipocytes were treated with RSG (Figure 2D). Importantly,
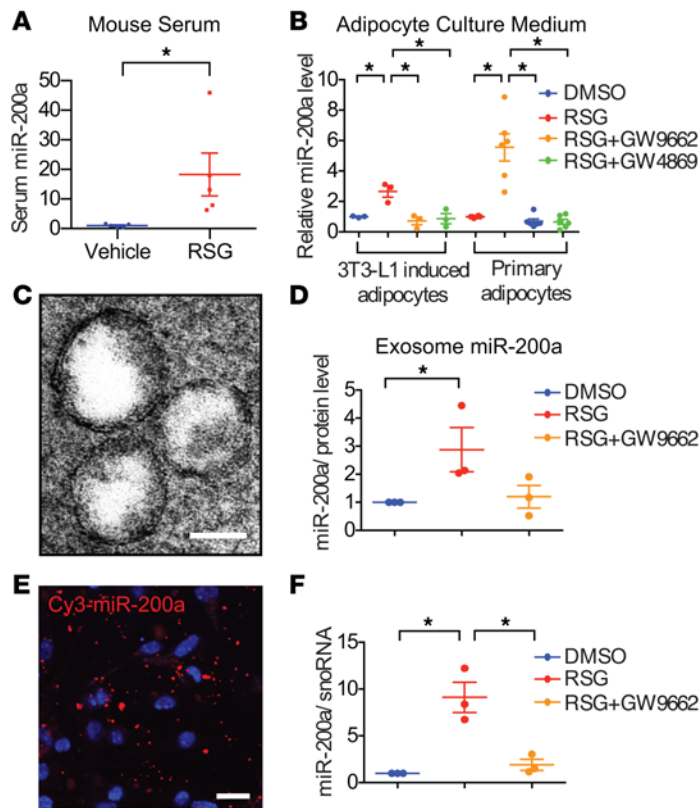
Figure 2. Exosome-dependent miR-200a secretion from adipocytes. (**A**) The levels of miR-200a were quantified using quantitative real-time PCR (qRT-PCR) in sera from mice treated with rosiglitazone (RSG) or vehicle (control). Note that miR-200a was increased after RSG treatment, but not in the vehicle control. $n = 5$ mice. (**B**) Expression levels of miR-200a were quantified using qRT-PCR in culture media from either 3T3-L1–induced adipocytes or mouse primary adipocytes treated with RSG alone, RSG and GW9662 (PPARγ antagonist), RSG and GW4869 (exosome biogenesis inhibitor), or DMSO (control). Note that RSG increased miR-200a levels in the culture media, but this effect was ablated when cells were treated with either PPARγ antagonist or exosome biogenesis inhibitor. The experiment was replicated 3–6 times. (**C**) Representative transmission electron micrographs of adipocyte-derived exosomes. The experiment was replicated 3 times. Scale bar: 50 nm. (**D**) Levels of miR-200a in exosomes were quantified using qRT-PCR from culture media of adipocytes treated with RSG alone, RSG and GW9662 (PPARγ antagonist), or DMSO (control). Note the increase in exosomal miR-200a levels when adipocytes were treated with RSG, but this effect was ablated when adipocytes were treated with PPARγ antagonist. The experiment was replicated 3 times. (**E**) Cardiomyocytes were incubated with exosomes derived from 3T3-L1 cells transfected with Cy3-conjugated miR-200a and were subsequently fixed and imaged. DAPI is depicted in blue; Cy3-miR-200a in red. Note that cardiomyocytes took up the miR-200a–containing exosomes. The experiment was replicated 3 times. Scale bar: 20 μm. (**F**) Levels of miR-200a were quantified using qRT-PCR of cardiomyocytes that were incubated with exosomes derived from treated adipocytes, as in **D**. Note that levels of miR-200a in cardiomyocytes increased after incubation with exosomes derived from RSG-treated adipocytes, but levels were not increased after incubation with exosomes derived from adipocytes treated with RSG and PPARγ antagonist. The experiment was replicated 3 times. snoRNA 202 and cel-miR-39 were used as internal controls for qRT-PCR experiments. Data are represented as mean ± SEM; *$P < 0.05$ according to 2-tailed Student's t test for **A** and 1-way ANOVA for **B**, **D**, and **F**.

increased levels of miR-200a in response to RSG were attenuated by addition of the PPARγ agonist GW9662.

Our earlier observations suggested that increased miR-200a in cardiac tissue was through an indirect mechanism (Figure 1, C and D). To test whether miR-200a could be from adipocyte-derived exosomes, we transfected a synthetic miR-200a (a 22-oligomer labeled with Cy3 fluorophore [Cy3-miR-200a]) into 3T3-L1–differentiated adipocytes. Exosomes from adipocyte culture media were collected after 24 hours and were used to treat cultured cardiomyocytes. As expected, we were able to detect Cy3-miR-200a in cardiomyocytes (Figure 2E). Incubation of cardiomyocytes with exosomes derived from adipocytes treated with RSG led to increased levels of miR-200a in cardiomyocytes. The effect was abrogated by GW9662 (Figure 2F). Taken together, these results suggested that adipocytes secreted miR-200a–containing exosomes could be delivered into cardiomyocytes, likely accounting for the increased level of mature miR-200a in the cardiomyocytes.

Exosomes transport functional miR-200a from adipocytes to cardiomyocytes. After establishing that purified exosomes containing miR-200a could be taken up by cardiomyocytes, we next wanted to establish a more in vivo–like situation in which we could coculture adipocytes with cardiomyocytes. In this setup, 3T3-L1 cells were seeded and induced to become adipocytes, followed by the addition of mouse neonatal cardiomyocytes in a Transwell chamber above the adipocytes (Figure 3A). The two cell types were separated by a membrane with a 0.4-μm pore size to prevent cell-cell contact or transfer of vesicles larger than 0.4 μm. First, we transfected adipocytes with Cy3-miR-200a and analyzed the Cy3 fluorescence in cardiomyocytes after 24 hours of coculture. In agreement with our earlier observations, we found that Cy3-miR-200a was indeed able to be transferred from adipocytes to cardiomyocytes during coculture (Figure 3C). Furthermore, to confirm that adipocytes were able to secrete miRNAs in exosomes that would subsequently be taken up by cardiomyocytes, we transfected adipocytes with a miRNA that is only naturally expressed in *Caenorhabditis elegans* (cel-miR-39). Analysis of cel-miR-39 levels in cardiomyocytes after transfection demonstrated that cardiomyocytes could take up cel-miR-39 from adipocytes. By using the exosome biogenesis inhibitor GW4869 we were able to attenuate the transfer of cel-miR-39 from adipocytes to cardiomyocytes, which was consistent with our earlier observations (Figure 3B).

To demonstrate that adipocytes were the source of miR-200a, we cultured cardiomyocytes in the presence or absence of adipocytes and added RSG to the culture media. In the absence of adipocytes, we observed no increase in miR-200a levels, consistent with our previous finding (Figure 1E). However, we observed a dramatic increase in cardiomyocyte miR-200a levels by RSG stimulation when cocultured with adipocytes. This effect could be inhibited by pretreating adipocytes with either the PPARγ antagonist GW9662 or the exosome biogenesis inhibitor GW4869. Unchanged pri-miR-200a levels in cardiomyocytes following treatment with RSG further confirmed that adipocytes were the source of miR-200a (Figure 3E).
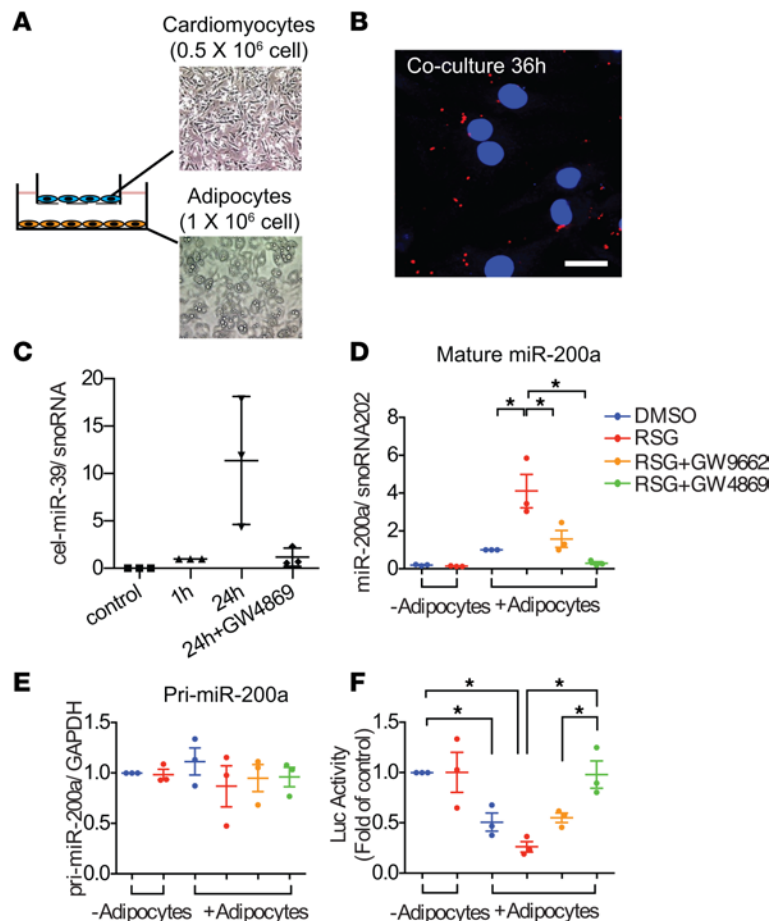
Figure 3. miR-200a is transported from adipocytes to cardiomyocytes in exosomes. (**A**) An in vitro coculture system was used in which cardiomyocytes are seeded in the top compartment, which is separated by a porous membrane from adipocytes that are cultured in the bottom of the plate. (**B**) Adipocytes were transfected with Cy3-miR-200a and cocultured with cardiomyocytes. After 24 hours, cardiomyocytes were fixed and imaged. DAPI is depicted in blue; Cy3-miR-200a in red. Note that the cardiomyocytes were able to take up the Cy3-conjugated miR-200a. The experiment was replicated 3 times. Scale bar: 20 μm. (**C**) Adipocytes were transfected with cel-miR-39 or not transfected (control) and subsequently seeded in the bottom compartment, as shown in **A**. RNA was isolated from cardiomyocytes at the indicated times after the start of the coculture. The levels of cel-miR-39 were quantified using quantitative real-time PCR (qRT-PCR). Note that cel-miR-39 was found in cardiomyocytes at 1 hour and 24 hours after coculture, and levels of cel-miR-39 were decreased when exosome biogenesis was inhibited by GW4869. The experiment was replicated 3 times. (**D** and **E**) Primary adipocytes were treated with rosiglitazone (RSG) alone, RSG and GW9662, or RSG and GW4869. Cardiomyocytes were subsequently cocultured in the presence or absence of the primary adipocytes for 48 hours. Expression levels of miR-200a (**D**) and pri-miR-200a (**E**) in cardiomyocytes were quantified using qRT-PCR. Note that mature miR-200a levels were increased only in cardiomyocytes that were cocultured in the presence of adipocytes. Pretreatment of adipocytes with RSG further augmented the levels of mature miR-200a. Importantly, this effect was rescued by treating cells with either PPARγ antagonist or exosome biogenesis inhibitor. The experiment was replicated 3 times. (**F**) Primary adipocytes were treated with RSG alone, RSG and GW9662, or RSG and GW4869. H9C2 cells were transfected with a miR-200a luciferase reporter construct and subsequently seeded in the upper compartment of the plate, as depicted in **A**. Luciferase activity of H9C2 cells was quantified after 48 hours of coculture. Note that luciferase levels were reduced in H9C2 cells when cocultured with adipocytes. This effect was exacerbated when adipocytes were pretreated with RSG and was rescued by treating cells with the PPARγ antagonist GW9662 and exosome biogenesis inhibitor GW4869. The experiment was replicated 3 times. snoRNA 202 was used as internal controls for qRT-PCR experiments. Data are represented as mean ± SEM; *P < 0.05 according to 1-way ANOVA.

After establishing the source of miR-200a, we determined whether secreted miR-200a was functional. We transfected H9C2 cells with a miR-200a reporter vector, consisting of 4 seed-binding sequences in the 3ʹ-UTR of a luciferase reporter gene. A reduction in luciferase activity is indicative of functional miR-200a, as miR-200a binds to the 3ʹ-UTR of luciferase and decreases its expression. Transfected H9C2 cells were seeded in the presence and absence of adipocytes, and luciferase activity in H9C2 cells was monitored after 72 hours. Luciferase activity in H9C2 cells was substantially reduced only following coculture with adipocytes. As expected, RSG treatment led to a further reduction in luciferase activity. This effect could be attenuated by pretreating adipocytes with the exosome biogenesis inhibitor GW4869 (Figure 3D) or by the PPARγ antagonist GW9662 (Figure 3F). In summary, these results demonstrated that functional mature miR-200a is packaged in secretory exosomes that could be transferred from adipocytes to cardiomyocytes to mediate gene silencing.

Adipocyte-derived miR-200a induces cardiomyocyte hypertrophy in vitro. Recent evidence shows that RSG treatment results in cardiac hypertrophy in both mouse and rat models (7–11). Given our data that show that RSG treatment leads to the secretion of functionally active miR-200a from adipocytes to cardiomyocytes, we hypothesized that miR-200a might target specific genes in cardiomyocytes that regulate cardiac hypertrophy. To uncover potential miR-200a target genes involved in cardiac hypertrophy, we took a bioinformatic approach to reveal *TSC1* as a putative candidate gene (Figure 4A). TSC1 has previously been shown to regulate cardiomyocyte size and cardiac remodeling through the mTOR pathway (32–34). Specifically, mice that have had TSC1 ablated in cardiomyocytes develop cardiac hypertrophy that leads to heart failure. This effect can be rescued by treating mice with the mTOR inhibitor rapamycin (35). TSC1 combines with TSC2 and functions as a GAP. The GTP-bound form of the G protein Rheb activates mTOR, and the TSC1/TSC2 complex converts Rheb to the GDP-bound form, thus inhibiting activation of mTOR (32). RSG-induced heart remodeling is associated with mTOR activation (10). We hypothesized that, if *TSC1* were a target of miR-200a, a consequent reduction in GAP activity of the TSC1/TSC2 complex would lead to increased activation of Rheb and subsequent activation of the hypertrophic mTOR pathway in cardiomyocytes. To test whether *TSC1* was a target of miR-200a, we constructed a luciferase reporter construct conjugated to the 3ʹ-UTR region of *TSC1* (Figure 4A). We cotransfected 293 cells with the reporter construct, a miR-200a mimic, or scrambled control. Only cotransfection with the miR-200a mimic reduced luciferase activity, showing that miR-200a was able to specifically target *TSC1* (Figure 4B). Next, we wanted to test the potential biological function
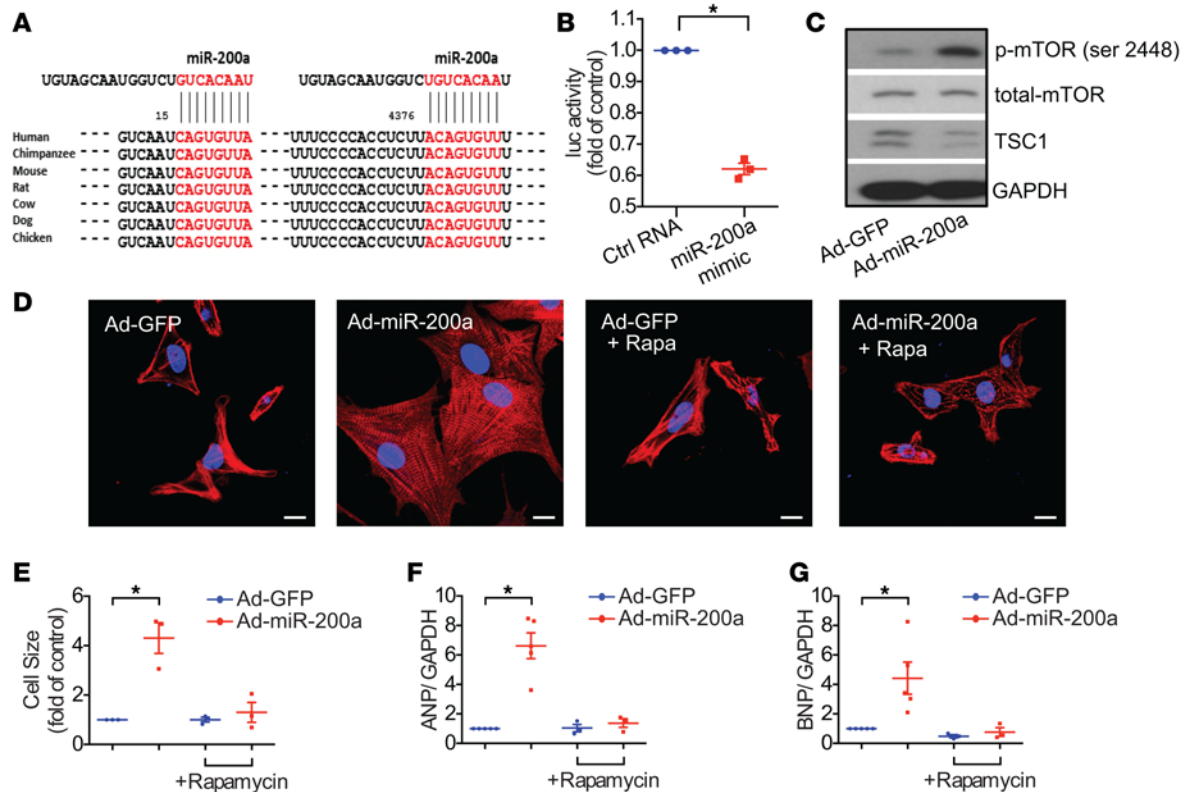
Figure 4. miR-200a activates the mTOR pathway to promote cardiomyocyte hypertrophy. (**A**) Comparison of the seed region of miR-200a with putative target sequences of the 3′-UTR conserved regions in human, chimpanzee, mouse, rat, dog, and chicken TSC1 mRNA. (**B**) HEK293 cells were cotransfected with either miR-200a mimic or scrambled RNA oligo (control) in combination with a TSC1 3′-UTR-luciferase reporter construct. Note that the luciferase activity was significantly reduced in cells expressing the miR-200a mimic compared with the control RNA oligo. The experiment was replicated 3 times. (**C**) Neonatal rat cardiomyocytes were infected with miR-200a or GFP (control) adenovirus, and the levels of phosphorylated mTOR (S2448), total mTOR, and TSC1 were detected. Note that the levels of phosphorylated mTOR increased and the levels of TSC1 decreased in miR-200a–overexpressing cells. The experiment was replicated 3 times. (**D** and **E**) Neonatal rat cardiomyocytes were infected with miR-200a or GFP (control) adenovirus, as in **C**, and were subsequently treated with or without rapamycin. Cells were fixed and stained for DNA using DAPI (blue) and Phalloidin (red) after 36 hours. Note that cell size increased when infected with miR-200a adenovirus, and this effect was reversible when cells were treated with the mTOR inhibitor rapamycin (Rapa). The experiment was replicated 3 times. Scale bar: 10 μm. (**F** and **G**) Neonatal rat cardiomyocytes were infected with miR-200a or GFP (control) adenovirus, as in **C**, and were treated with or without rapamycin. RNA was isolated from cells and levels of cardiac hypertrophy markers atrial natriuretic peptide (*Anp*) and B-type natriuretic peptide (*Bnp*) were quantified using quantitative real-time PCR. Note that levels of both *Anp* and *Bnp* increased when cells were infected with miR-200a, and this was reversible when treated with rapamycin. The experiment was replicated 5 times. Data are represented as mean ± SEM; *$P < 0.05$ according to 2-tailed Student's *t* test for **B** and 1-way ANOVA for **E**–**G**.

of miR-200a on TSC1 levels and mTOR signaling in cardiomyocytes. Given the low transfection efficiency observed with cardiomyocytes using conventional transfection methods, we generated miR-200a and GFP (control) adenoviruses. Thirty-six hours following viral infection, levels of TSC1 and both total and phosphorylated mTOR were quantified. miR-200a overexpression marked reduced protein levels of TSC1 and increased mTOR phosphorylation (Figure 4C). Furthermore, when cardiomyocyte size was measured, cells overexpressing miR-200a were significantly larger than control GFP-treated counterparts (Figure 4, D and E). This effect was dependent on mTOR signaling, because treatment with the mTOR inhibitor rapamycin rendered cells insensitive to miR-200a–induced hypertrophy (Figure 4, D and E). Cardiac remodeling is often accompanied by reexpression of a fetal gene program (12). Indeed, both atrial natriuretic peptide (*Anp*) and B-type natriuretic peptide (*Bnp*) levels significantly increased when cardiomyocytes were treated with miR-200a. Treatment with the mTOR inhibitor rapamycin was sufficient to block the response of cardiomyocytes to miR-200a–induced hypertrophy (Figure 4, F and G).

After establishing that miR-200a was able to affect TSC1 levels and mTOR signaling in isolated cardiomyocytes, we sought next to identify whether miR-200a secreted from adipocytes could have similar functional consequences in cardiomyocytes. To study this, we employed our coculture system to study effects of RSG-treated adipocytes on cardiomyocytes and found that RSG-treated adipocytes
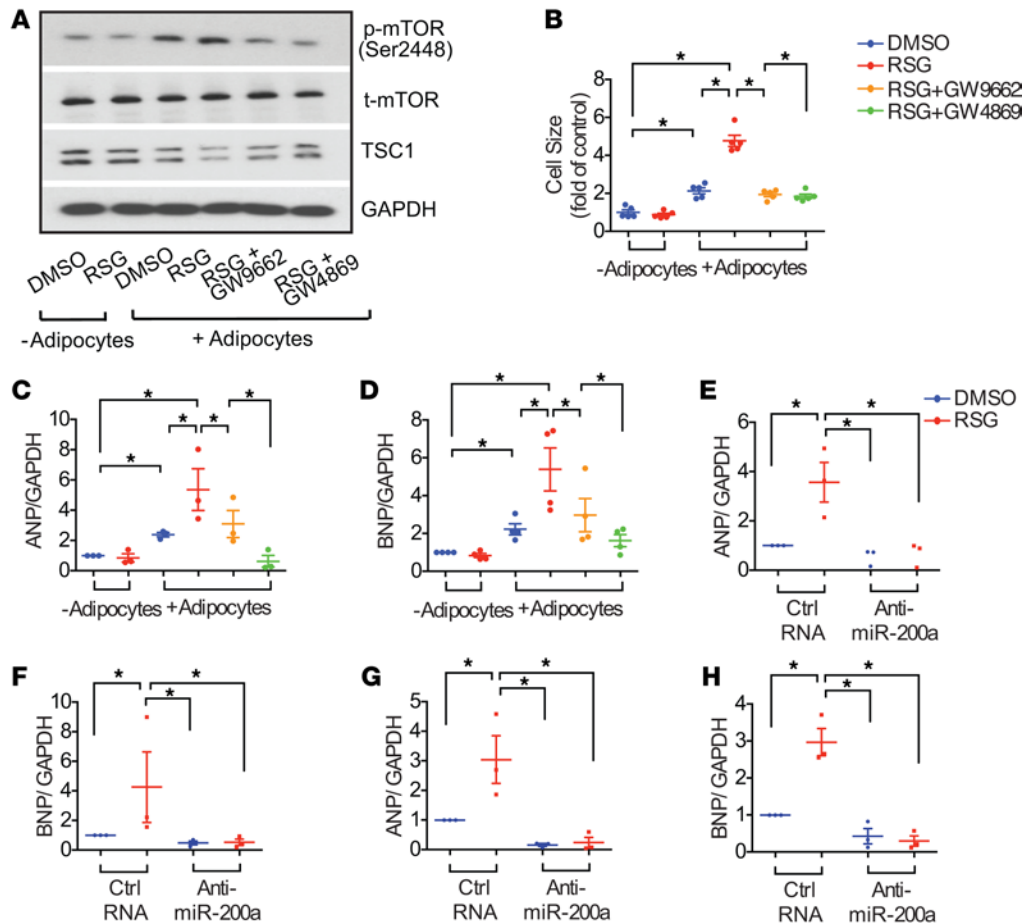
Figure 5. Adipocyte-derived miR-200a mediates cardiomyocyte hypertrophy in vitro. (**A**) Primary adipocytes were treated with rosiglitazone (RSG) alone, RSG and GW9662 (PPARγ antagonist), or RSG and GW4869 (exosome biogenesis inhibitor). Cardiomyocytes were subsequently cocultured in the presence or absence of the primary adipocytes for 72 hours, as in Figure 4A. Cardiomyocytes were subsequently lysed, and Western blots were performed. Note that in the absence of adipocytes, levels of TSC1, total mTOR, and phosphorylated mTOR in cardiomyocytes were unaffected when treated with RSG. Conversely, in the presence of adipocytes, RSG activated mTOR signaling and decreased protein levels of TSC1. Importantly, this effect was rescued using either PPARγ antagonist or exosome biogenesis inhibitor. The experiment was replicated 4 times. (**B–D**) Adipocytes and cardiomyocytes were cocultured and treated as in **A**, and RNA was subsequently extracted after 72 hours. The cell size and levels of atrial natriuretic peptide (*Anp*) and B-type natriuretic peptide (*Bnp*) in cardiomyocytes were quantified. Note that the cell size and levels of *Anp* and *Bnp* increased when cocultured with adipocytes, and this effect was exacerbated when treated with RSG. This effect was rescued by treating adipocytes with PPARγ antagonist and exosome biogenesis inhibitor. The experiment was replicated 3–5 times. (**E** and **F**) 3T3-L1–induced adipocytes were transfected with either miR-200a antagomir or control RNA for 24 hours followed by treatment with RSG or DMSO (control). Cardiomyocytes were subsequently cocultured, and RNA was extracted and quantified using quantitative real-time PCR after 72 hours of coculture. Note that the increased levels of *Anp* and *Bnp* were ablated when adipocytes were treated with miR-200a antagomir. The experiment was replicated 3 times. (**G** and **H**) Rat cardiomyocytes were infected with miR-200a antagomir or control RNA for 24 hours before being adenovirus cocultured with adipocytes. Adipocytes were treated with RSG and RNA was isolated from cardiomyocytes. Note the increased levels of *Anp* and *Bnp* were ablated when cardiomyocytes were treated with miR-200a antagomir. The experiment was replicated 3 times. Data are represented as mean ± SEM; *$P < 0.05$ according to 1-way ANOVA.

reduced levels of TSC1 and increased mTOR activity in cardiomyocytes (Figure 5A). These effects were abrogated by treatment with either the PPARγ antagonist GW9662 or the exosome biogenesis inhibitor GW4869. To confirm that cardiomyocytes were actively undergoing remodeling, we examined the cell size and levels of *Anp* and *Bnp* in the presence and absence of adipocytes. As expected, the cell size and levels of both were elevated only when cardiomyocytes were cocultured with adipocytes (Figure 5, B–D). RSG treatment further increased the cell size and the levels of *Anp* and *Bnp*, and this effect was attenuated either by antagonism of PPARγ signaling or inhibition of exosome biogenesis.

To evaluate the functional role of adipocyte-derived miR-200a in promoting hypertrophy in cardiomyocytes, we used a miR-200a antagomir to specifically inhibit miR-200a function. Adipocytes were transfected with a miR-200a antagomir (Figure 5, E and F), or cardiomyocytes were infected with a miR-200a
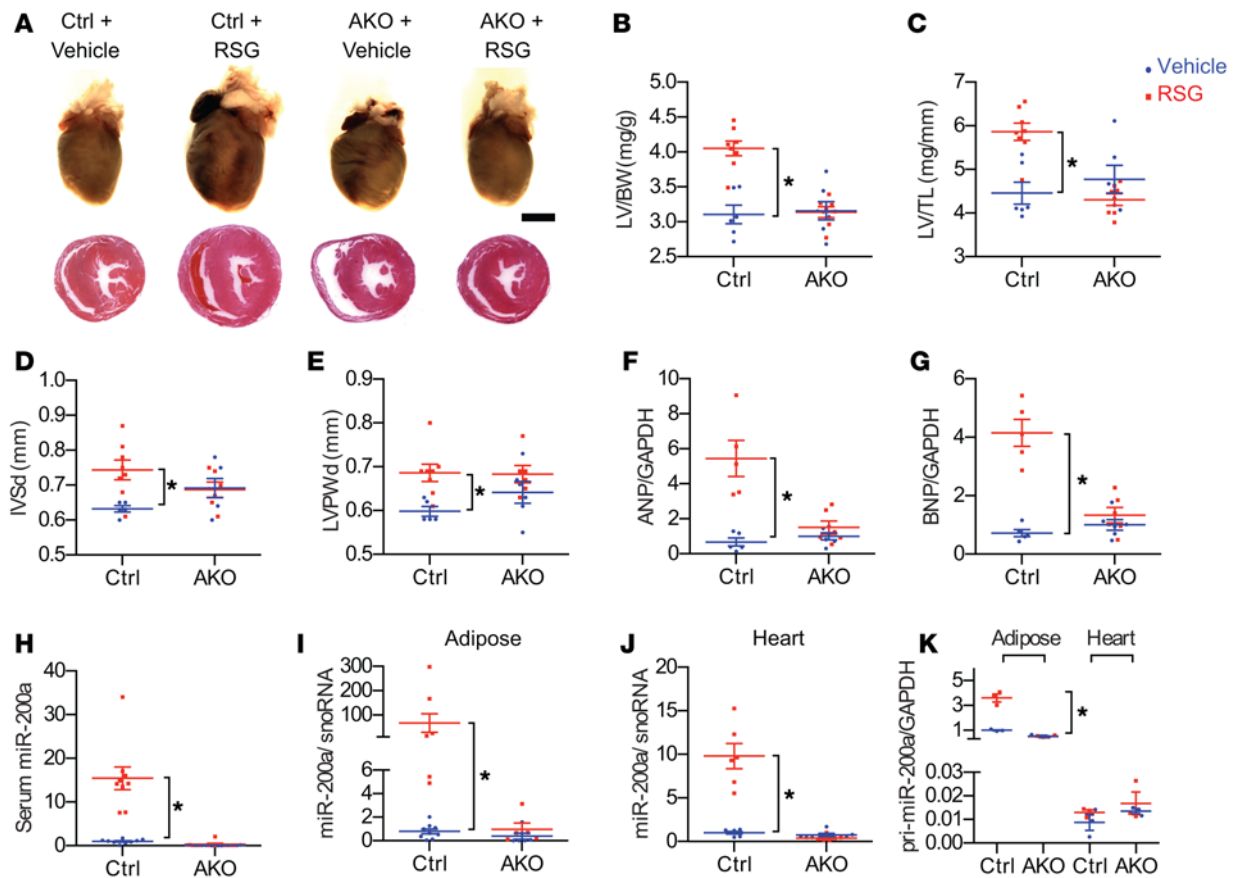
Figure 6. Rosiglitazone-induced cardiac hypertrophy is attenuated in mice with PPARγ-deficient adipocytes. Adipose-specific PPARγ knockout (AKO) and littermate control mice (Ctrl) were treated with rosiglitazone (RSG) to induce cardiac hypertrophy. (**A**) Representative whole-mouse heart (top) and H&E-stained sections (bottom). Scale bar: 2 mm. *n* = 3 mice per group. (**B** and **C**) The ratios of left ventricle weight (LV) to body weight (BW) and LV to tibia length (TL) were measured. Note that both ratios increased in the control mice; however, the effect was blunted in the AKO mice. *n* = 5–8 mice. (**D** and **E**) Echocardiography revealed thicknesses of the interventricular septum (IVSd) and left ventricular posterior wall (LVPWd). Note that both septal and posterior wall thicknesses increased in the control mice, but this effect was not observed in AKO mice. *n* = 5–8 mice. (**F** and **G**) RNA from the left ventricle was extracted, and levels of atrial natriuretic peptide (*Anp*) and B-type natriuretic peptide (*Bnp*) were quantified using quantitative real-time PCR (qRT-PCR). Note that *Anp* and *Bnp* increased in control mice but were unaffected in AKO mice. *n* = 5 mice. (**H–K**) RNA was extracted from serum, adipose tissue, and cardiac tissue from AKO and control mice, and levels of mature miR-200a (**H–J**) or pri-miR-200a (**K**) were analyzed using qRT-PCR. Note that RSG increased levels of miR-200a in tissues from control mice, whereas RSG failed to increase the level of miR-200a in serum, adipose tissue, and cardiac tissue in AKO mice. Pri-miR-200a was only increased in adipose tissue from RSG-treated WT mice. *n* = 5–8 per group. Data are represented as mean ± SEM; *$P < 0.05$ according to 1-way ANOVA.

antagomir–expressing adenovirus (Figure 5, G and H). Cells were then cocultured and treated with RSG. In both cell types, treatment with the miR-200a antagomir abolished effects of RSG on cardiac hypertrophy markers *Anp* and *Bnp*, indicating that RSG acted through miR-200a to induce cardiomyocyte hypertrophy. Taken together, these data suggested that miR-200a was necessary and sufficient to target *TSC1* in cardiomyocytes, leading to stimulation of the mTOR pathway and cardiomyocyte hypertrophy.

RSG-induced cardiac hypertrophy is attenuated in mice with PPARγ-deficient adipocytes. To test our hypothesis that RSG activates PPARγ signaling in adipocytes, leading to secretion of miR-200a–containing exosomes, which in turn induces cardiomyocyte hypertrophy, we used an adipose-specific PPARγ knockout mouse (AKO mouse), utilizing *Fabp4*-Cre and a floxed allele of PPARγ. We treated mice with RSG for 4 weeks and assessed levels of PPARγ target genes in cardiac and adipose tissue. RSG was able to induce known target genes *Ap2* and *Cd36* in cardiac tissue of AKO mice; however, RSG failed to induce target gene expression in adipose tissue, demonstrating the specificity of the knockout (Supplemental Figure 3, A–D). Histological analyses and measurement of left ventricle weight/body weight ratios and left ventricle weight/tibia length ratios revealed a blunted hypertrophic response to RSG in AKO mice when compared with control mice (Figure 6, A–C), supporting our in vitro observations. Further echocardiographic analysis following

RSG treatment revealed that interventricular septal wall thickness at end diastole and left ventricle posterior wall thickness at end diastole were also attenuated in AKO mice compared with littermate control mice (Figure 6, D and E, and Table 1). Furthermore, both *Anp* and *Bnp* levels were blunted in cardiac tissue from AKO mice in response to RSG treatment (Figure 6, F and G). We next examined levels of miR-200a in sera and adipose and cardiac tissue from AKO and control mice (Figure 6, H–J). While levels of miR-200a significantly increased in all samples from control littermates following RSG treatment, no increases in levels of miR-200a were observed in AKO mice. Levels of pri-miR-200a were significantly upregulated only in adipose tissue, but not in cardiac tissue, of control WT mice and were not upregulated in either adipose or cardiac tissue in AKO mice (Figure 6K). The foregoing data were consistent with the hypothesis that adipose tissue is a major source of circulating and cardiac miR-200a and that PPARγ signaling in adipose tissue is essential for cardiac hypertrophy in response to RSG treatment.

Discussion

There is an overall consensus that significant crosstalk occurs between adipose and cardiac tissue, but until now molecular players have remained elusive. Here, we reveal a direct signaling axis between adipocytes and cardiomyocytes that is guided by exosomal delivery of miR-200a. We show that PPARγ activation in adipose tissue leads to expression and release of miR-200a in exosomes into the circulatory system. Subsequently, miR-200a–containing exosomes target cardiomyocytes, in which miR-200a suppress expression of TSC1 and stimulates mTOR signaling to induce cardiac hypertrophy.

Secretion of exosomes has emerged as an important paracrine mechanism for regulation of cardiac hypertrophy between cardiac fibroblasts and cardiomyocytes. For example, a recent study showed that cardiomyocytes are able to take up exosomes containing miR-21* that are secreted by cardiac fibroblasts, leading to cardiomyocyte hypertrophy by targeting *SORBS2*, SH3 domain–containing protein 2, and enigma homolog in cardiomyocytes (23). However, delivery of exosomes to cardiomyocytes from other organs has proven elusive until now. In the present study, we provide in vitro evidence that miR-200a was transported in exosomes from adipocytes to cardiomyocytes, in which it targeted genes involved in regulating the mTOR pathway. However, direct evidence of adipocyte-derived exosomes after RSG treatment as mediators of cardiac hypertrophy remains to be established in vivo. In addition, it is very likely that there are other mediators in adipocyte-derived exosomes after RSG treatment. Further studies are needed to identify these potential mediators.

miR-200a is abundantly expressed in adipose tissue, whereas it is barely expressed in vessels and heart at basal conditions (Supplemental Figure 1). Upon PPARγ activation, miR-200a transcription in adipose tissue, as measured by the levels of pri-miR-200a, is activated about 6 folds, while levels of pri-miR-200a in heart remain at basal levels. The exact mechanism for the observation remains to be determined, but it could be due to a lack of an essential cofactor(s) in the heart that functions together with PPARγ to activate miR-200a transcription. Alternatively, it could be because of a lack of a transcriptional repressor(s) that is restricted to the heart and is not present in adipose tissue that allows miR-200a transcription activation specifically in adipose tissue. It is interesting to note that miR-200a is upregulated in response to oxidative stress and in animal models of diabetes (36). Epidemiological studies show that diabetes and insulin resistance are powerful predictors of cardiovascular morbidity and mortality and are independent risk factors for death in patients with established heart failure (37–39). Animal models of diabetes also show signs of cardiac hypertrophy (40). Our data imply that miR-200a might be secreted from adipose tissue and transported in exosomes that may target cardiac tissue and contribute to diabetic cardiomyopathy.

In this study, we identified TSC1, a repressor of mTOR signaling, as a target of miR-200a inhibition. Exogenous miR-200a overexpressed by adenovirus, or delivered by exosomes from adipocytes, downregulated TSC1 in recipient cardiomyocytes and enhanced mTOR activation, leading to cardiomyocyte hypertrophy (Figure 4). Transfection of an antagomir to miR-200a in adipocytes or cardiomyocytes was sufficient to attenuate hypertrophy (Figure 5). TSC1 has previously been shown to regulate cardiomyocyte size and cardiac remodeling through the mTOR pathway (32–34). It has been shown that mice in which TSC1 is specifically ablated in cardiomyocytes develop cardiac hypertrophy that leads to heart failure (35). Our data indicated a critical role for miR-200a in targeting TSC1 to result in cardiac hypertrophy. However, miRNAs function by complementary pairing of their seed regions to 3ʹ-UTRs of target mRNAs, and miR-200a has many potential targets in heart. Other examples of miR-200a targets include *FOG2* (friend of GATA 2) and *SIRT1* (silent information regulator 1) (41–44). SIRT1 is expressed in cardiomyocytes and has been shown to play a cardioprotective role following ischemia/reperfusion injury (45). FOG2 is a multitype zinc finger

protein that interacts with GATA factors and is essential for heart development and cardiac function. Cardiomyocyte-specific deletion of FOG2 leads to postnatal heart failure (46). In addition, FOG2 also directly binds to p85α, the regulatory subunit of PI3K, and interferes with the formation of the PI3K complex. As an inhibitor of PI3K/Akt pathway, decreased FOG2 expression can activate PI3K/Akt signaling (41), which has a well-established role in cardiac hypertrophy (47–49). Specific roles of SIRT1 and/or FOG2 in PPARγ activation–induced cardiac hypertrophy remain to be determined.

PPARγ is most highly expressed in adipose tissue and is also expressed at low levels in other tissues (1). Experiments with tissue-specific overexpression or knockout of PPARγ have been crucial in helping dissect specific effects of PPARγ activity in different tissues. For example, mice with cardiac-specific overexpression of PPARγ develop cardiomyopathy, suggesting a prohypertrophic action of PPARγ in heart (13). However, mice with cardiomyocyte-specific ablation of PPARγ develop hypertrophy in response to RSG (7), implying that systemic PPARγ activation causes cardiac hypertrophy through non-cardiomyocytes. Our data demonstrated that RSG activated PPARγ signaling in adipose tissue to indirectly lead to cardiac remodeling. Other examples highlighting PPARγ crosstalk between different tissues include activation of PPARγ in brain, which contributes to thiazolidinedione-induced weight gain and whole-body energy balance (50). Additionally, PPARγ regulated adiponectin from adipocytes improves endothelial function in diabetic mice (51).

Adipose tissue is an important endocrine organ that plays a cardioprotective role by reducing lipotoxic effects in other peripheral tissues and by maintaining a healthy balance of critical adipokines (15). Our data suggest that secretion of exosomes from adipocytes is essential for induction of cardiac hypertrophy in response to RSG, as inhibition of exosome synthesis completely normalized *Anp* and *Bnp* mRNA levels (Figure 5, B and C). Notably, only a partial restoration of normal *Anp* and *Bnp* mRNA levels was observed when PPARγ signaling was inhibited, implying that there are other factors in exosomes that can regulate cardiac hypertrophy independently of PPARγ signaling. This is perhaps unsurprising, because many factors are likely to be secreted in exosomes from adipose tissue. For example, a recent microarray study revealed that mRNA and miRNAs other than miR-200a are found in exosomes derived from adipocytes (18). Factors other than oligonucleotides may also play a role. For example, recent studies have shown that, in response to inflammatory stimuli, adipocytes secrete exosomes containing the proteins MFG-E8 and RBP4 (52).

In conclusion, our data suggest that one of the direct links between PPARγ activation in adipocytes and cardiomyocyte hypertrophy is through mir-200a. However, the in vivo role of miR-200a in the adipocyte-cardiomyocyte axis remains to be determined. Our data suggest that exosome-mediated communication may have important clinical consequences in adipose biology and cardiomyopathy in the setting of obesity.

Methods

Additional details are provided in the Supplemental Experimental Procedures.

Animals and RSG treatment. C57 BL/6 mice (strain code: 027) were purchased from Charles River. *Fabp4*-Cre [B6.Cg-Tg (*Fabp4*-cre) 1 Rev/J, stock no. 005069] and *PPARG* flox (B6.129-Ppargtm2Rev/J, stock no. 004584) mice were purchased from The Jackson Laboratory.

Fabp4-Cre mice (Cre driven by fatty acid–binding protein 4 [*Fabp4*] promoter) were crossed with floxed *PPARG* mice to obtain adipocyte-specific PPARγ-knockout (AKO) mice (homozygous floxed *PPARG* and *Fabp4*-Cre positive). AKO mice were bred with homozygous floxed *PPARG* mice to generate both AKO mice and littermate control mice (homozygous floxed *PPARG* and *Fabp4*-Cre negative) (53).

Male mice (8 to 10 weeks of age, 6 to 8 mice per group) were treated with either regular chow or RSG chow for 4 weeks. RSG chow (0.01% RSG, Cayman Chemical) was produced by mixing RSG compound with D10012G rodent chow (Research Diet). Daily food consumption was 0.1 g chow/10 g body weight per day, which delivers a RSG dose of 10 mg/kg body weight per day.

Echocardiographic studies. Mice were anesthetized with 1% isoflurane and underwent echocardiography using a Vevo 2100 ultrasound system (VisualSonics, SonoSite FUJIFILM) with a 32- to 55-MHz linear transducer. Measurements of heart rate (HR), left ventricular end-diastolic dimensions and left ventricular end-systolic dimensions, end-diastolic interventricular septal thickness, and left ventricle posterior wall thickness were determined from the left ventricle M-mode tracing. Percentage of fractional shortening was used as an indicator of systolic cardiac function. n = 6–8 mice were used for each group.

Cardiac hypertrophy calculation and histology. Mice were anesthetized with ketamine/xylazine and weighed to determine total body weight. Hearts were removed and left ventricles were weighed. Tibias

were dissected and measured. Left ventricular weight to body weight ratios (mg per g) and/or left ventricular weight to tibia length ratios (mg per mm) were used as indicators of cardiac hypertrophy. Hearts were fixed in PFA, dehydrated in 70% EtOH, and embedded in paraffin. Paraffin-embedded cardiac sections (8-μm thick) were stained with H&E as previously described (54). All chemicals were from Sigma-Aldrich.

Cell culture. Primary neonatal cardiomyocytes were isolated by using the Neonatal Cardiomyocyte Isolation System (Worthington) according to the manufacturer's instructions and were maintained in 80% DMEM/20% M199 medium supplemented with 10% horse serum, 5% FBS, and 1% penicillin/streptomycin, with Brdu (100 μM) and ArAc (10 μM). Male Sprague-Dawley rats or C57BL/6 mice were used to extract primary cultures of mature adipocytes. Briefly, epididymal fat pads were removed, minced, and digested with type I collagenase (Worthington) as described previously (55). Murine 3T3-L1 fibroblasts (a gift of Jerrold M. Olefsky's laboratory, Department of Medicine, UCSD) were passaged in DMEM containing 10% fetal calf serum (FCS). 3T3-L1 preadipocytes were differentiated into adipocytes when confluent by adding differentiation medium (DMEM containing 10% FBS, 1.0 μM dexamethasone, 0.5 mM methylisobutylxanthine, 1.0 μg/ml insulin). After 2 days, the cells were transferred to adipocyte growth medium (DMEM containing 10% FBS, 1.0 μg/ml insulin) and fed every other day. Differentiation to mature adipocytes was confirmed by Oil Red O staining of lipid vesicles (56). 3T3-L1–differentiated adipocytes and primary adipocytes were treated with RSG (Cayman Chemical), GW9662 (Cayman Chemical), and GW4869 (Cayman Chemical) at the concentration 1 μM, 5 μM and 20 μM, respectively. Other reagents were from Sigma-Aldrich unless specified.

Coculture experiments. 3T3-L1 cells (1×10^6/well) were seeded into 6-well plates and induced into mature adipocytes before the coculture experiment. Primary neonatal cardiomyocytes (0.5×10^6) were seeded into the well inserts (0.4-μm diameter pore, Corning) and cultured in complete cardiomyocyte culture medium 24 hours before coculture experiments. Before starting the coculture experiments, both adipocytes and cardiomyocytes were washed with PBS. All coculture experiments were done in serum-free DMEM.

RNA isolation and quantitative RT-PCR. RNA was extracted from cultured cells or exosomes by using the TRIzol reagent (Life Technologies) according to the manufacturer's instructions. For the isolation of miRNAs from serum or condition medium samples, 5 pg of synthetic *C. elegans* miRNA cel-miR-39 was added to each sample as a spike-in control for purification efficiency, and RNA was extracted using the miRNeasy Serum/Plasma Kit (Qiagen) following the manufacturer's instructions. Serum or conditioned medium was centrifuged at 2000 *g* for 10 minutes to remove cells before RNA isolation. Isolated RNAs were reverse transcribed into complementary DNA by using the TaqMan primer sets for miRs (Applied Biosystems) or Oligo (dT) primers for mRNAs. Real-time PCR was performed with the TaqMan Fast Universal PCR Master Mix (Applied Biosystems) or iQ SYBR Green Supermix (Bio-Rad) by using the TaqMan probes (Applied Biosystems) or specific primer pairs. Mature miR expression levels were normalized to the control snoRNA202 or Cel-miR-39 probes. Expression of mRNAs were normalized to *Gapdh*. Other PCR primers are listed in Supplemental Table 2.

Western blot analysis. Total protein was isolated from mouse hearts or neonatal rat cardiomyocytes, run on 4%–12% SDS-PAGE gel (Life Technologies), and transferred overnight on to PVDF membrane. Blots were blocked and incubated with the indicated primary antibodies, washed, probed with use of horseradish peroxidase–conjugated secondary antibodies in rabbit (1:5,000) or mouse (1:2,000) (Dako), and visualized by the ECL chemiluminescence system. Antibodies used for immunofluorescence and Western blotting are listed in Supplemental Table 1.

Immunofluorescence. Cardiomyocytes were fixed with 4% PFA, permeabilized with Triton X-100 (0.1%), and stained with phalloidin using Rhodamine-conjugated Phalloidin (Cytoskeleton) according to the manufacturer's instructions. After staining, the samples were visualized by confocal microscopy (Olympus FV-1000).

Transfection and reporter assay. 3T3-L1 adipocytes were transfected with cel-miR-39 (10 nM final concentration) or miR-200a antagomir (50 nM final concentration) (mirVan miRNA Inhibitors, Ambion) using Lipofectamine RNAiMAX (Life Technologies) according to the manufacturer's instructions. For luciferase assays, the luciferase reporter constructs containing the full-length TSC1 3˅-UTR (cloned from HEK293 genomic DNA) or 4x(ACAGTGTTA) "seed" binding sequences of miR-200a from the 3˅-UTR of pri-miR-reporter vector (Ambion) were used. HEK293 cells were cotransfected using Lipofectamine 2000 (Life Technologies) with luciferase reporter plasmid DNA and miR-200a mimic (5 nM) or control oligonucleotide (Life Technologies) as per manufacturer's recommendations. Twenty-four hours after transfection, luciferase activity was measured using the Luciferase assay system (Promega) and normalized to β-galactosidase activity assessed using o-nitrophenyl-β-D-galactopyranoside (Sigma-Aldrich).

Adenovirus. miR-200a overexpression and antagomir adenoviruses were constructed by Welgen Inc. Briefly, mouse pri-miR-200a cDNA or miR-200a antagomir sequences (5ˇ-ACATCGTTACCAGACAGT-GTTA-3ˇ) were cloned into pENT-CMV or pEQU6 vectors, respectively. The pENT-pri-miR-200a cDNA and pEQU6-antagomir were treated with LR Clonase II enzyme (Life Technologies) and ligated into the pAd-REP plasmid that contains the remaining adenovirus genome. The recombination products were amplified in *E. coli* (JM109 strain), and cosmid DNA was purified. The purified cosmid DNA (2 μg) was digested with Pac1 and transfected into HEK293 cells with Lipofectamine 2000 (Life Technologies) according to manufacturer's instructions. HEK293 cells were grown in 10% FBS DMEM and adenovirus plaques were seen 7 days after transfection. Empty pEntCMV shuttle vector or scramble RNA inserted in pEQU6 served as the respective controls.

Exosome isolation. Exosomes were purified as described previously (29). Briefly, conditioned media from cultured adipocytes were subjected to sequential centrifugation steps of 300 *g*, 2,000 *g*, and 10,000 *g* before exosomes were pelleted at 100,000 *g* for 3 hours. Supernatant was discarded, and exosomes were washed and resuspended in PBS.

TEM experiment. Exosome were fixed (2% paraformaldehyde, 2% glutaraldehyde in 0.15 M sodium cacodylate buffer, pH 7.4) and stained overnight in 1% osmium tetroxide, 0.8% potassium ferrocyanide. The following day, exosomes were stained for 2 hours in 2% uranyl acetate and subsequently dehydrated in a series of ethanol and acetone washes. Exosomes were embedded in Durcupan resin (EMD), and ultrathin sections (60–70 nm) were stained with lead citrate. Electron micrographs were recorded using a JEOL 1200EX electron microscope operated at 80 kV. All chemicals were from Sigma-Aldrich.

Statistics. Data are expressed as mean ± SEM and were examined by using 2-tailed Student's *t* test or ANOVA for comparisons among groups as indicated. $P < 0.05$ was considered statistically significant.

Study approval. All animal procedures were performed in accordance with National Institutes of Health guidelines and were approved by the UCSD Animal Care and Use Committee. UCSD has an Animal Welfare Assurance (A3033-01) on file with the Office of Laboratory Animal Welfare and is fully accredited by AAALAC International.

Author contributions

XF, MJS, KO, LF, JZ, NDD, YG, TW, KLP, and HDH performed the research; XF, JC, and NW designed the research; and XF, MJS, JC, and NW wrote the manuscript.

Acknowledgments

Address correspondence to: Ju Chen, 9500 Gilman Drive M/C 0613C, La Jolla, California 92093, USA. Phone: 858.822.4276; E-mail: juchen@ucsd.edu. Or to: Nanping Wang, The Advanced Institute for Medical Sciences, Dalian Medical University, Dalian, 116044, China. Phone: 86.041186110233; E-mail: nanpingwang2003@yahoo.com.

1. Ahmadian M, et al. PPARγ signaling and metabolism: the good, the bad and the future. *Nat Med*. 2013;19(5):557–566.
2. Lehrke M, Lazar MA. The many faces of PPARgamma. *Cell*. 2005;123(6):993–999.
3. Kung J, Henry RR. Thiazolidinedione safety. *Expert Opin Drug Saf*. 2012;11(4):565–579.
4. Nissen SE, Wolski K. Effect of rosiglitazone on the risk of myocardial infarction and death from cardiovascular causes. *N Engl J Med*. 2007;356(24):2457–2471.
5. Home PD, et al. Rosiglitazone evaluated for cardiovascular outcomes in oral agent combination therapy for type 2 diabetes (RECORD): a multicentre, randomised, open-label trial. *Lancet*. 2009;373(9681):2125–2135.
6. Soccio RE, Chen ER, Lazar MA. Thiazolidinediones and the promise of insulin sensitization in type 2 diabetes. *Cell Metab*. 2014;20(4):573–591.
7. Duan SZ, Ivashchenko CY, Russell MW, Milstone DS, Mortensen RM. Cardiomyocyte-specific knockout and agonist of peroxi-

some proliferator-activated receptor-gamma both induce cardiac hypertrophy in mice. *Circ Res*. 2005;97(4):372–379.

8. Arakawa K, Ishihara T, Aoto M, Inamasu M, Kitamura K, Saito A. An antidiabetic thiazolidinedione induces eccentric cardiac hypertrophy by cardiac volume overload in rats. *Clin Exp Pharmacol Physiol*. 2004;31(1-2):8–13.

9. Chang CS, et al. Diuretics prevent thiazolidinedione-induced cardiac hypertrophy without compromising insulin-sensitizing effects in mice. *Am J Pathol*. 2014;184(2):442–453.

10. Festuccia WT, et al. Rosiglitazone-induced heart remodelling is associated with enhanced turnover of myofibrillar protein and mTOR activation. *J Mol Cell Cardiol*. 2009;47(1):85–95.

11. Liu Y, et al. Metabonomic profiling revealed an alteration in purine nucleotide metabolism associated with cardiac hypertrophy in rats treated with thiazolidinediones. *J Proteome Res*. 2013;12(12):5634–5641.

12. Heineke J, Molkentin JD. Regulation of cardiac hypertrophy by intracellular signalling pathways. *Nat Rev Mol Cell Biol*. 2006;7(8):589–600.

13. Son NH, et al. Cardiomyocyte expression of PPARgamma leads to cardiac dysfunction in mice. *J Clin Invest*. 2007;117(10):2791–2801.

14. He H, et al. Rosiglitazone causes cardiotoxicity via peroxisome proliferator-activated receptor γ-independent mitochondrial oxidative stress in mouse hearts. *Toxicol Sci*. 2014;138(2):468–481.

15. Turer AT, Hill JA, Elmquist JK, Scherer PE. Adipose tissue biology and cardiomyopathy: translational implications. *Circ Res*. 2012;111(12):1565–1577.

16. Lin Q, et al. Activation of hypoxia-inducible factor-2 in adipocytes results in pathological cardiac hypertrophy. *J Am Heart Assoc*. 2013;2(6):e000548.

17. Rosen ED, Spiegelman BM. What we talk about when we talk about fat. *Cell*. 2014;156(1-2):20–44.

18. Ogawa R, et al. Adipocyte-derived microvesicles contain RNA that is transported into macrophages and might be secreted into blood circulation. *Biochem Biophys Res Commun*. 2010;398(4):723–729.

19. He L, Hannon GJ. MicroRNAs: small RNAs with a big role in gene regulation. *Nat Rev Genet*. 2004;5(7):522–531.

20. Topkara VK, Mann DL. Role of microRNAs in cardiac remodeling and heart failure. *Cardiovasc Drugs Ther*. 2011;25(2):171–182.

21. Wei Y, et al. Multifaceted roles of miR-1s in repressing the fetal gene program in the heart. *Cell Res*. 2014;24(3):278–292.

22. Callis TE, et al. MicroRNA-208a is a regulator of cardiac hypertrophy and conduction in mice. *J Clin Invest*. 2009;119(9):2772–2786.

23. Bang C, et al. Cardiac fibroblast-derived microRNA passenger strand-enriched exosomes mediate cardiomyocyte hypertrophy. *J Clin Invest*. 2014;124(5):2136–2146.

24. Creemers EE, Tijsen AJ, Pinto YM. Circulating microRNAs: novel biomarkers and extracellular communicators in cardiovascular disease? *Circ Res*. 2012;110(3):483–495.

25. Mitchell PS, et al. Circulating microRNAs as stable blood-based markers for cancer detection. *Proc Natl Acad Sci U S A*. 2008;105(30):10513–10518.

26. Chen X, et al. Characterization of microRNAs in serum: a novel class of biomarkers for diagnosis of cancer and other diseases. *Cell Res*. 2008;18(10):997–1006.

27. Valadi H, Ekström K, Bossios A, Sjöstrand M, Lee JJ, Lötvall JO. Exosome-mediated transfer of mRNAs and microRNAs is a novel mechanism of genetic exchange between cells. *Nat Cell Biol*. 2007;9(6):654–659.

28. Hergenreider E, et al. Atheroprotective communication between endothelial cells and smooth muscle cells through miRNAs. *Nat Cell Biol*. 2012;14(3):249–256.

29. Zhuang G, et al. Tumour-secreted miR-9 promotes endothelial cell migration and angiogenesis by activating the JAK-STAT pathway. *EMBO J*. 2012;31(17):3513–3523.

30. Zhang Y, et al. Secreted monocytic miR-150 enhances targeted endothelial cell migration. *Mol Cell*. 2010;39(1):133–144.

31. Zhou J, et al. Regulation of vascular smooth muscle cell turnover by endothelial cell-secreted microRNA-126: role of shear stress. *Circ Res*. 2013;113(1):40–51.

32. Huang J, Manning BD. The TSC1-TSC2 complex: a molecular switchboard controlling cell growth. *Biochem J*. 2008;412(2):179–190.

33. Lee CH, Inoki K, Guan KL. mTOR pathway as a target in tissue hypertrophy. *Annu Rev Pharmacol Toxicol*. 2007;47:443–467.

34. Gao XM, et al. Inhibition of mTOR reduces chronic pressure-overload cardiac hypertrophy and fibrosis. *J Hypertens*. 2006;24(8):1663–1670.

35. Malhowski AJ, et al. Smooth muscle protein-22-mediated deletion of Tsc1 results in cardiac hypertrophy that is mTORC1-mediated and reversed by rapamycin. *Hum Mol Genet*. 2011;20(7):1290–1305.

36. Reddy MA, et al. Pro-inflammatory role of microrna-200 in vascular smooth muscle cells from diabetic mice. *Arterioscler Thromb Vasc Biol*. 2012;32(3):721–729.

37. Battiprolu PK, Gillette TG, Wang ZV, Lavandero S, Hill JA. Diabetic Cardiomyopathy: Mechanisms and Therapeutic Targets. *Drug Discov Today Dis Mech*. 2010;7(2):e135–e143.

38. Kannel WB, Hjortland M, Castelli WP. Role of diabetes in congestive heart failure: the Framingham study. *Am J Cardiol*. 1974;34(1):29–34.

39. Rubler S, Dlugash J, Yuceoglu YZ, Kumral T, Branwood AW, Grishman A. New type of cardiomyopathy associated with diabetic glomerulosclerosis. *Am J Cardiol*. 1972;30(6):595–602.

40. Battiprolu PK, et al. Metabolic stress-induced activation of FoxO1 triggers diabetic cardiomyopathy in mice. *J Clin Invest*. 2012;122(3):1109–1118.

41. Hyun S, et al. Conserved microRNA miR-8/miR-200 and its target USH/FOG2 control growth by regulating PI3K. *Cell*. 2009;139(6):1096–1108.

42. Eades G, Yao Y, Yang M, Zhang Y, Chumsri S, Zhou Q. miR-200a regulates SIRT1 expression and epithelial to mesenchymal transition (EMT)-like transformation in mammary epithelial cells. *J Biol Chem*. 2011;286(29):25992–26002.

43. Liu M, et al. Resveratrol inhibits mTOR signaling by promoting the interaction between mTOR and DEPTOR. *J Biol Chem*. 2010;285(47):36387–36394.

44. Ghosh HS, McBurney M, Robbins PD. SIRT1 negatively regulates the mammalian target of rapamycin. *PLoS ONE*. 2010;5(2):e9199.

45. Hsu CP, et al. Silent information regulator 1 protects the heart from ischemia/reperfusion. *Circulation*. 2010;122(21):2170–2182.

46. Zhou B, et al. Fog2 is critical for cardiac function and maintenance of coronary vasculature in the adult mouse heart. *J Clin Invest*. 2009;119(6):1462–1476.

47. Shiojima I, et al. Disruption of coordinated cardiac hypertrophy and angiogenesis contributes to the transition to heart failure. *J Clin Invest*. 2005;115(8):2108–2118.

48. Matsui T, et al. Phenotypic spectrum caused by transgenic overexpression of activated Akt in the heart. *J Biol Chem*. 2002;277(25):22896–22901.

49. Walsh K. Akt signaling and growth of the heart. *Circulation*. 2006;113(17):2032–2034.

50. Lu M, et al. Brain PPAR-γ promotes obesity and is required for the insulin-sensitizing effect of thiazolidinediones. *Nat Med*. 2011;17(5):618–622.

51. Wong WT, et al. Adiponectin is required for PPARγ-mediated improvement of endothelial function in diabetic mice. *Cell Metab*. 2011;14(1):104–115.

52. Deng ZB, et al. Adipose tissue exosome-like vesicles mediate activation of macrophage-induced insulin resistance. *Diabetes*. 2009;58(11):2498–2505.

53. Sugii S, et al. PPARgamma activation in adipocytes is sufficient for systemic insulin sensitization. *Proc Natl Acad Sci U S A*. 2009;106(52):22504–22509.

54. Sheikh F, et al. Mouse and computational models link Mlc2v dephosphorylation to altered myosin kinetics in early cardiac disease. *J Clin Invest*. 2012;122(4):1209–1221.

55. Marshall S, Garvey WT, Geller M. Primary culture of isolated adipocytes. A new model to study insulin receptor regulation and insulin action. *J Biol Chem*. 1984;259(10):6376–6384.

56. van Harmelen V, Skurk T, Hauner H. Primary culture and differentiation of human adipocyte precursor cells. *Methods Mol Med*. 2005;107:125–135.